New solar hybrid absorption / thermochemical refrigeration cycle

***J. Fitó*[a], S. Mauran[b,c], D. Stitou[b], N. Mazet[b], A. Coronas[a]**

[a] *CREVER, Dep. of Mechanical Engineering, Universitat Rovira i Virgili, Av. Països Catalans, 26, ES-43007 Tarragona, Spain. jaume.fito@estudiants.urv.cat;alberto.coronas@urv.cat*

[b] *PROMES-CNRS, UPR 8521, Laboratoire Procédés, Matériaux et Energie Solaire, Rambla de la Thermodynamique, Tecnosud, 66100 Perpignan, France. mauran@univ-perp.fr ; stitou@univ-perp.fr ; mazet@univ-perp.fr*

[c] *Université de Perpignan Via Domitia (UPVD). Av. Paul Alduy 52, 66860 Perpignan - France. mauran@univ-perp.fr*

Abstract:

In this work, a new solar hybrid absorption / thermochemical refrigeration cycle with intrinsic storage capacity is proposed and described. In this cycle, both the absorption and the thermochemical subcycles provide the refrigeration effect, and in addition, the thermochemical subcycle provides storage capability with high energy density and nearly zero energy losses in the storage period. Along with the proposed configuration, several possible working pairs are reviewed. Furthermore, adequate performance indicators are defined for the cycle, and a preliminary simulation is carried out to give an idea about the cycle's advantages.

Keywords:

Hybrid systems, Absorption, Thermochemical storage, Performance indicators, Solar thermal refrigeration.

1. Introduction

Renewable energy sources are increasingly regarded as the solution to greenhouse gas emissions in the recent decades. The availability of abundant and free energy sources becomes more attractive as state-of-the-art technologies improve. Specially, solar energy is one of the most promising.

Efficient solar systems need to cope with the lack of simultaneity, known as 'mismatch', between the available solar radiation (which is intermittent) and the demand of energy. Sensible heat storage is a common solution [1], but it is not very energetic efficient, because of the large volumes required, and the thermal losses, especially in mid- and long-term storage periods. Latent heat storage reduces heat losses, but still does not offer enough energy density.

Thermochemical systems are a promising option for solar applications [2]. As well as viability for refrigeration applications, they intrinsically offer energy storage, with high energy density (thus reducing the system's size) and virtually no losses, for long periods of time [3-5]. Supplied energy to the system remains stored as chemical potential. These systems offer good storing possibilities, although they show low COP values (due to issues in heat transfer to solid phase). Thus, it is an interesting idea to combine a thermochemical storage system with a refrigeration cycle.

Absorption refrigeration technology is commercially available. Various configurations exist and development is still ongoing. Solar absorption refrigeration has also been studied [6], being the energy storage issue a strong barrier against improvement. Attaching a thermochemical system to it can provide efficient energy storage, and the possibility of continuous operation even if using an intermittent heat source, aiming to an eventually autonomous off-grid operation.

In this work, a new solar hybrid cycle is proposed and described, in a more compact and economic design than just driving both systems separately.

2. Cycle description

The proposed cycle is shown in Fig. 1. Its configuration is similar to a conventional absorption cycle, but with an added reactor (R) for the thermochemical subsystem. Both the thermochemical and the absorption subsystems can share the same condenser (C) and evaporator (E) only if they use the same fluid as refrigerant. If the refrigerant was different in each subsystem, an additional condenser and evaporator would be necessary for the thermochemical subcycle, and they should work separately from the absorption subcycle. Selecting the same refrigerant (F) for both subsystems is the most practical decision, since the global system becomes more compact.

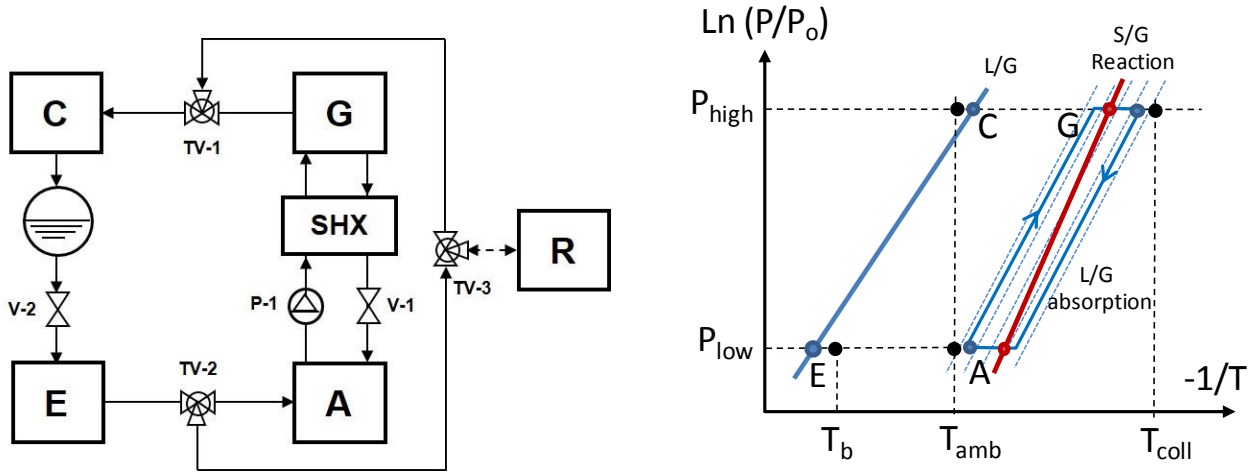

Fig. 1. Hybrid absorption / thermochemical cycle.

Connections between the absorption subsystem and the reactor are made by three-way valves (TV-1 and TV-2), which allow to select which subsystem is working (they can also operate at the same time in certain situations; read below). The global system can be operated continuously even when there is no heat source available, as long as there is enough energy stored by the thermochemical subsystem. The connection R <-> TV-3 is showed as a dashed line to indicate that the stream in it can flow in either direction, depending on the mode in which the subsystem is operating.

The absorption subsystem works the same way as a conventional absorption chiller. The generator (G) receives heat (Q_G) from the solar collector to regenerate the sorbent. Refrigerant vapor condenses at the condenser, rejecting condensation heat (Q_C). The regenerated sorbent goes to the absorber (A), to absorb the refrigerant vapor and release absorption heat (Q_A). In the evaporator, the refrigerant evaporates, removing heat (Q_E), being this the useful effect of the refrigeration cycle. The solution heat exchanger (SHX) improves the system's overall efficiency.

The thermochemical subsystem [7] is formed by the condenser (C), the evaporator (E) and a reactor (R) in which occurs a solid/gas reaction written in its generic form as:

$$\langle MX.\mu F\rangle + \nu(F) \leftrightarrow \langle MX.(\mu+\nu)F\rangle + \nu.\Delta h_r \qquad (1)$$

with <MX> being a solid reactive salt having fixed μ or (μ+ν) moles of gas (F) per mole of salt. Note that the stoichiometric coefficient μ may be zero.

The two salts <MX.μF> and <MX.(μ+ν)F>, and the vapor (F) constitute a monovariant system, i.e. at a given pressure, fixed by the condenser or the evaporator, the equilibrium temperature of the reaction is fixed whatever the mole proportion of the two salts. That is a first great difference with the absorption system which is bivariant.

Moreover the transformation of reactor is intrinsically non-stationary, the composition of the reactive salt evolving between <MX.μF> and <MX.(μ+ν)F>. The sense of the reaction depends on the constraint temperature applied to the reactor at a given pressure. For a constraint temperature lower than the equilibrium one, the reaction evolves from left to right in the expression (1). In this

case the reaction is exothermic and the heat released at the constraint temperature is $\nu.\Delta h_r$ for one mole of salt. Inversely for a higher temperature than the equilibrium one, the reaction evolves from right to left and is endothermic.

A full thermochemical subsystem cycle includes two different main stages and two secondary ones:

- During the first main stage, the reactor is connected to the condenser which imposes the operating pressure. The refrigerant fluid F is desorbed from the reactor, which requires consumption of the heat of reaction ($Q_r \propto \nu.\Delta h_r$) provided by the high temperature heat source. After condensing, the refrigerant is stored in liquid form in a reservoir at the outlet of the condenser. This stage will be hereinafter referred as 'charge stage' (see Fig. 2), as it enables the solar energy storage in the chemical products.
- During the second main stage the reactor is connected to the evaporator (E) which fixes again a low operating pressure. The vaporized refrigerant is absorbed by the reactor, releasing the same heat of reaction (Q_r) to the heat sink, for example at ambient temperature. Conversely to the previous stage, this one will be referred as 'discharge stage' (see Fig. 3), as it is responsible for providing the useful cooling effect (Q_{cold}) at the required temperature (T_b) by consuming the previously stored chemical energy.
- Between the two main stages the reactor is disconnected from the condenser or evaporator. The connection via the heat exchange fluid is changed from the high temperature heat source towards the low temperature heat sink or reciprocally. These secondary stages involve sensible heat stored that is approximately recovered by the reactor. So in a first approximation they do not affect the coefficient of performance (hereinafter defined) of this thermochemical subsystem.

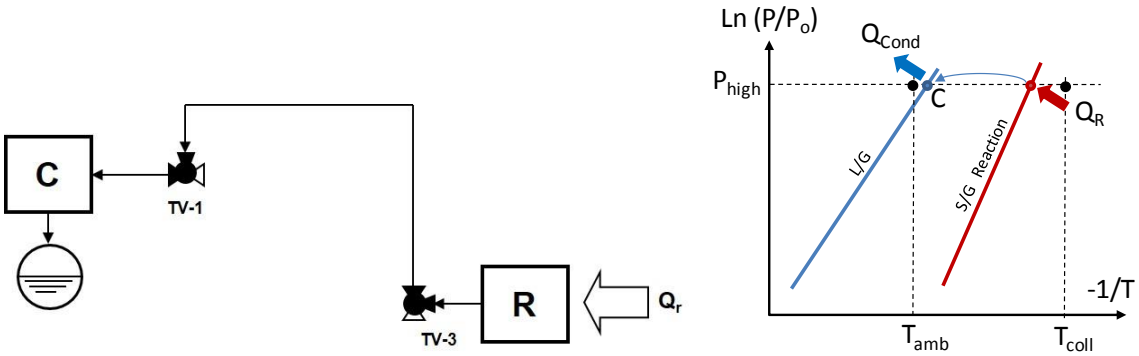

Fig. 2. Regeneration stage (charge stage) in the thermochemical subcycle.

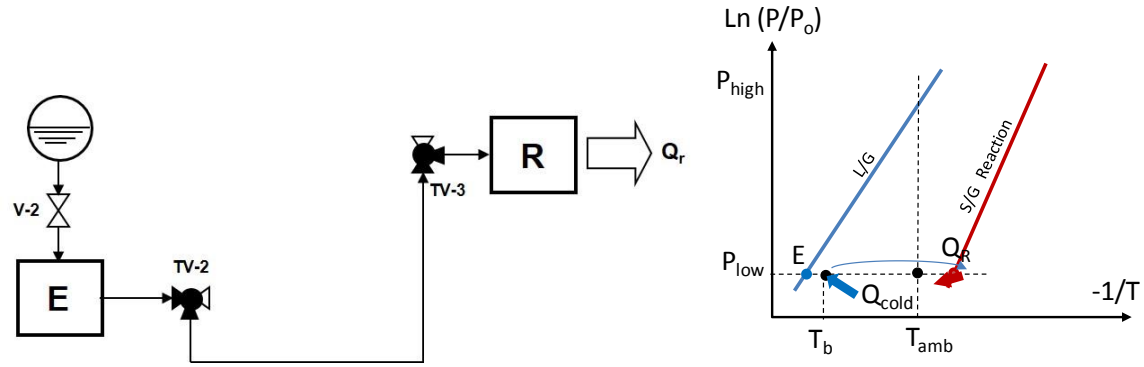

Fig. 3. Discharge stage in the thermochemical subsystem (stored energy being utilized).

All possible operation scenarios for the system are considered in Table 1. Operation or not-operation of the absorption subsystem (ABS) and the thermochemical subsystem (TCH) is indicated

in relation to the availability of source heat (Q_{in}), the demand of cooling (Q_{need}) and the maximum possible cooling output from the absorption subsystem with the given heat input ($Q_{E,max}^{ABS}$).

The simplest case (case #1) takes place when there is no source heat available and there is no heat demand either; such situation could happen in applications where refrigeration is not always needed, like domestic room cooling, and in that case neither the absorption subsystem nor the thermochemical one would be required to operate.

Table 1. Characterization of all possible operation scenarios for the hybrid ABS/TCH system.

#	Q_{in}	Q_{need}	ABS	$\left(Q_{E,max}^{ABS} - Q_{need}\right)$	TCH	Notes
1	= 0	= 0	OFF	= 0	OFF	No source (Q_{in}), no demand (Q_{need}), systems off
2	> 0	= 0	OFF	> 0	*CHARGE*	Source, no demand -> Storage
3	> 0	> 0	*ON*	> 0	*CHARGE*	Source exceeds demand -> Storage
4	> 0	> 0	*ON*	= 0	OFF	Source equals demand
5	> 0	> 0	*ON*	< 0	*DISCHARGE*	Source insufficient to cover demand -> TCH on
6	= 0	> 0	OFF	< 0	*DISCHARGE*	Demand, no source -> TCH on
0*	= 0	> 0	*ON**	< 0	OFF	Demand, no source, no stored energy -> Auxiliary source

Cases #2 to #5 (included) show the behavior of the subsystems when there is solar heat available and different situation occur with relation to the demand: with no load (#2), the ABS subsystem is not operating and the TCH system is in "CHARGE" mode; with load, and extra source heat available (#3), both the ABS and the TCH subsystem are operating, the latter one in "CHARGE" mode; when there is load and it is exactly satisfied by the absorption effect, with no surplus heat remaining (#4), the ABS subsystem is ON and the TCH subsystem is OFF (this case is not likely to happen for a long time period in a realistic operation scenario); when there is load and the absorption subsystem alone cannot satisfy it (#5), and there is stored energy in the TCH subsystem, the TCH subsystem is operating in discharge mode (ON). Finally, case #6 indicates that when there is cooling demand but no source heat available, and there is stored energy, the ABS subsystem is OFF and the TCH one is ON.

In case #0, there is a cooling load to satisfy, but no source heat available, and in addition, there is no energy stored in the TCH subsystem. In this situation, the use of another, stable and permanently available heat source would be required, most likely a non-renewable heat source; the operation would be carried out by the ABS subsystem, and the TCH part would be OFF. However, depending on the demand and availability profiles, and the system design, this situation might be avoided.

3. Working Pairs

In this section, some possible working pairs for the cycle are reviewed. The selection process depends on some considerations.

Since both subcycles have to share the same refrigerant, it is crucial for both of them that only pure refrigerant can be circulated to the condenser/evaporator segment. For the absorption subcycle, this excludes the possibility of using the well-known ammonia/water working pair for this configuration, unless a rectification system was added, which would reduce the overall system's performance and increase its cost, therefore making the machine less attractive. Instead, other working pairs are available which use ammonia as refrigerant and a sorbent which will not vaporize in the generator, such as the ammonia/lithium nitrate ($NH_3/LiNO_3$) and the ammonia/sodium thiocyanate (NH_3/NaSCN) pairs.

The application will also reduce the field of optimal working fluids for each case. In general, while combinations with ammonia as refrigerant may be used for refrigeration purposes like food conservation, or other applications which require to produce cold at under zero degrees, working pairs using water as refrigerant are recommendable for space conditioning in large buildings, since in that kind of application does not require very low temperatures in the evaporator. The abovementioned working pairs can be used in the absorption subcycle for cold production at very low temperatures, and when it comes to using water as refrigerant, the traditional and also well-known water/lithium bromide (H_2O/LiBr) pair can be used, among other similar pairs.

Precisely for solar applications, an additional limitation is added by the solar collector system: although in theory high driving temperatures could be achieved by both the absorption and the thermochemical subcycle depending on the selected pairs, their practical use in solar applications is eventually limited by the highest reachable temperature at the solar collector. Moreover, increasing the temperature of the driving heat source has a negative impact on the cycle performance.

The location influences the selection of the working pair: locations with high ambient temperatures force the decision of using working fluids with accordingly high driving heat temperature.

Environmental and safety considerations are always to be taken into account: from this standpoint it would be preferable to use water as refrigerant, or in any case, non-toxic, non-flammable and non-contaminating fluids.

For solid-gas sorption systems, several choices are available for physical, thermochemical or composite sorption [8]. Regarding thermochemical sorption, conventional working pairs include: metal chloride/bromide/iodide-ammonia reactions, with driving temperatures ranging from 50 ^{0}C to 350 ^{0}C; metal oxides-oxygen/water/carbon dioxide reactions, with driving temperatures in the range of 150 ^{0}C-1000 ^{0}C; and metal hydrides-hydrogen reactions, with driving temperatures between 110 ^{0}C and 400 ^{0}C.

Regarding working pairs using ammonia as refrigerant in thermochemical systems, metal chlorides [9], bromides or iodides are commonly used. One of the most interesting ones is calcium chloride ($CaCl_2$) [10], and many others are available, such as barium chloride ($BaCl_2$) [11,12], strontium chloride ($SrCl_2$), or strontium bromide ($SrBr_2$) [13] as interesting ones.

4. System performance simulation

With the purpose of testing the cycle performance, a preliminary simulation of the cycle was carried out. Firstly, a profile for the demand of source heat was defined by the degree days method. Secondly, a simplified simulation model was built, and run for a given location and sun radiation profile. Simulation results are presented in this work with their corresponding discussion.

4.1. Definition of performance indicators

Performance assessment is a common and important issue when evaluating a system's potential, and especially when comparing it with other systems [14]. First Law Efficiency (η) and Coefficient of Performance (COP) are commonly used for evaluation of energy efficiency. However, in many cases, energetic considerations alone cannot fully characterize the system's performance [15], and when used without any additional indicator, they can result in misleading conclusions [16].

And added issue is observed in this particular cycle. Since it is originally conceived for solar applications, it will be discontinuously operated, and each one of the operation intervals will take place in transient regime. As a consequence, energy and exergy evaluations cannot be done in terms of power (like in stationary operation approaches), but in terms of energy instead. For a defined operating interval, this means that each form of energy rate going into or coming out from the cycle must be integrated for the whole time lapse to do the efficiency calculations.

Apart from energy and exergy, system evaluation can be done from other standpoints as well: economical and environmental are interesting ones. However, the aim of this work is to study the

viability of the system and to carry out a preliminary evaluation of its potential and interest. Therefore, other approaches for performance assessment will not be taken into account at this point.

4.1.1. Coefficient Of Performance (COP)

The COP of the system for a determined operation period was defined as the relation between the total useful refrigeration effect delivered at the evaporator and the total driving heat input to the cycle (pump work being neglected), as it can be seen in (2).

$$COP^{\xi} = \frac{\int_{t=t_0^{\xi}}^{t=t_n^{\xi}} \dot{Q}_E^{\xi}(t) \cdot dt}{\int_{t=t_0^{\xi}}^{t=t_n^{\xi}} \dot{Q}_{in}^{\xi}(t) \cdot dt} \qquad \{ \xi = [HYB,\ ABS,\ TCH] \} \tag{2}$$

This definition of COP shows two main differences with respect to the common general definition for the COP. The first one and most remarkable is the fact that it deals in terms of total energy instead of energy flow rate. The reason for this variation is the intrinsically discontinuous and transient operation of this type of cycle, as a consequence of being driven by an intermittent heat source. Since the driving heat provided to the cycle will not be constant in time, and the required refrigeration effect will be varying with time for the application considered in this study (residential cooling), performance calculations must be done by integration over the defined operation period.

The term Q_E^{ξ} corresponds to the refrigeration effect at the evaporator that is provided by the cycle under consideration, that is, the absorption subcycle, the thermochemical subcycle, or the hybrid global cycle, being the latter the sum of the two previous ones.

The term Q_{in}^{ξ} corresponds the driving heat input to the cycle under consideration: for the absorption part, it is the heat input to the generator, Q_G; for the thermochemical part, it is the heat input to the reactor, Q_{r1}; and for the global hybrid system, it is the sum of these two.

The values t_0^{ξ} and t_n^{ξ} correspond to the integration time limits for each subsystem.

4.1.2. Coefficient of Satisfaction of the Demand (*CSD*)

Although the COP shows performance by comparing the useful output to the heat input, it is also interesting to compare the output to the energy need in the application. A specific performance indicator, the Coefficient for Satisfaction of the Demand (CSD), is proposed for this system (3):

$$CSD^{\xi} = \frac{\int_{t=t_0^{\xi}}^{t=t_n^{\xi}} \dot{Q}_{need}(t) \cdot dt - \int_{t=t_0^{\xi}}^{t=t_n^{\xi}} \frac{\left[\dot{Q}_{need}(t) - \dot{Q}_E^{\xi}(t)\right]^2}{\dot{Q}_{need}(t)} \cdot dt}{\int_{t=t_0^{\xi}}^{t=t_n^{\xi}} \dot{Q}_{in}^{\xi}(t) \cdot dt} \qquad \{ \xi = [HYB,\ ABS] \} \tag{3}$$

with $\dot{Q}_{need}(t)$ the cooling power needed for the application.

According to this definition, it results that 0 ≤ CSD ≤ COP. If the cooling effect provided by the system ($\dot{Q}_E^{\xi}(t)$) equals the demand ($\dot{Q}_{need}(t)$), then CSD = COP. If the cooling effect is zero, then CSD = 0. In some manner, this indicator shows how, near to its nominal performance (COP), the system operates, according to which fraction of the load is satisfied.

The CSD definition can also be normalized to obtain 0 ≤ CSD ≤ 1 as an output, thus showing which fraction of the demand is satisfied (4).

$$CSD_{norm}^{\xi} = \frac{Q_{need} - \left[\int_{t=t_0}^{t_n} \frac{\left[\dot{Q}_{need}(t) - \dot{Q}_E^{\xi}(t)\right]^2}{\dot{Q}_{need}(t)} \cdot dt \right]}{Q_{need}} \qquad \{ \xi = [HYB,\ ABS] \} \tag{4}$$

with Q_{need} (= $\int_{t=t_0^{\xi}}^{t=t_n^{\xi}} \dot{Q}_{need}(t) \cdot dt$) the cooling energy required.

4.2. Cycle simulation procedure

Two main steps can be distinguished in the simulation procedure: estimation of a sample energy demand profile, and calculation of the cycle's operation.

4.2.1. Definition of the demand profile

The demand profile depends to a big extent on the application for which the cycle is selected. For the configuration which is presented in this work, the cycle is suitable for applications where refrigeration is needed. To show the strengths of the cycle proposed in this work, an application case of residential cooling has been chosen, since it has a clearly variable cooling demand profile, which can illustrate the mismatch between source heat and demand of cooling the cycle aims to solve. The demand of cooling for a sample residence has been determined on an hourly basis.

The hourly demand of cooling for a sample residence was determined by normalization of the monthly demand, through the degrees day method. This method has been proven to obtain very close-to-reality results among the simple methods [17], due to the considerable effect of the external environment temperature on the thermal demand.

According to this method, firstly the monthly demand of the building was determined as a function of its specific monthly demand and its useful floor area:

$$Q_{need,m} = q_{need,m} \cdot A_{floor} \tag{5}$$

Reference values for the specific demand of cooling for each type of building can be obtained from real measurements, specialized bibliography or simulation software [18].

Next step was the determination of the cooling degree days (CDD) for the entire month (6) and for each day (7), as a function of the difference between the hourly ambient temperatures ($T_{amb,h}$) and a base temperature for cooling (T_b). The former ones can be easily obtained from weather files available at several sources. The latter is a set point, normally fixed by each country's legislation.

$$CDD_m = \frac{\sum_{h=1}^{h=h_m} \left(T_{amb,h} - T_b\right)}{24} \qquad for\ T_{amb,h} > T_b \tag{6}$$

$$CDD_d = \frac{\sum_{h=1}^{h=h_d} \left(T_{amb,d} - T_b\right)}{24} \qquad for\ T_{amb,h} > T_b \tag{7}$$

After the cooling degree days for the month and for each day were known, the monthly demand of cooling was normalized to obtain the daily demand. Distinction between working days ($Q_{need,wd}$) and weekend days ($Q_{need,we}$) was made [19], as it can be seen in (8) and (9), respectively. Demand was assumed to be 50% higher during weekends, taken into account with the β_{we} factor. To keep the sum of both values being the total monthly demand (10), a redistribution factor (k_d) was adjusted.

$$Q_{need,wd} = k_d \cdot Q_{need,m} \cdot \frac{CDD_{wd}}{CDD_m} \tag{8}$$

$$Q_{need,we} = k_d \cdot \beta_{we} \cdot Q_{need,m} \cdot \frac{CDD_{we}}{CDD_m} \tag{9}$$

$$Q_{need,m} = \sum_m Q_{need,wd} + \sum_m Q_{need,we} \tag{10}$$

To convert from total daily demand to hourly demand (subscript "h") in a residential building, a utilization profile was selected where energy consumption is expressed on an hourly basis as a percentage of the total daily energy consumption. The hourly percentage of total daily consumption was expressed as a factor (α_h) and used to determine the hourly demand (11 and 12).

$$Q_{need,wd,h} = \alpha_h \cdot Q_{need,wd} \tag{11}$$

$$Q_{need,we,h} = \alpha_h \cdot Q_{need,we} \quad (12)$$

4.2.2. Simulation of the cycle

The simulation scenario was conceived as the hybrid cycle being connected to a solar thermal system, and satisfying the cooling demand of a residence. Hypotheses and parameters concerning the residence and the solar thermal system can be seen in Table 2.

Table 2. Assumed parameters for the cycle simulation.

Location	Barcelona
Date	July
Building type	Single-family residence
Building surface (m^2)	100
Monthly demand of cooling (MWh)	0.85
Base temperature for cooling (^{0}C)	21
Solar collector type	Flat plate
Collector slope	45º
Useful area of one collector (m^2)	2.3624
Solar thermal system efficiency	0.5

Generator and evaporator temperatures were assumed to be 90 ^{0}C and 5 ^{0}C, respectively. The system was assumed to have an auxiliary, stable heat source, to be used when the heat provided by the solar collectors is not enough to meet the demand, or when it is at too low temperature.

Since only a preliminary, not thermodynamic simulation was considered for this work, fixed COP values were assumed for both subcycles. For the absorption subcycle, a COP of 0.7 was used, which is an assumable value for the NH_3/NaSCN working pair, for instance, as can be seen in simulations from [20]; in the case of the thermochemical subcycle, a fixed COP value of 0.3 was used, which is assumable for pairs involving ammonia, for instance $NH_3/BaCl_2$ [3,21].

Information about hourly ambient temperature and solar radiation for the selected location was processed to obtain the hourly solar radiation on the collector field ($\dot{Q}_{rad}(t)$). With this value and having into account the global efficiency of the solar thermal system (η_{solar}), the hourly total driving heat input ($\dot{Q}_{in}(t)$) was determined (13).

$$\dot{Q}_{in}(t) = \dot{Q}_{rad}(t) \cdot \eta_{solar} \quad (13)$$

Then, calculations for each subcycle were made. The simulation procedure takes into consideration all cases described in Table 1. Given the input driving heat ($\dot{Q}_{in}(t)$) provided by the solar loop, the maximum deliverable amount of refrigeration effect by the absorption subcycle $\left(\dot{Q}_{E,\max}^{ABS}(t) = \dot{Q}_{in}(t) \cdot COP^{ABS}\right)$ is compared to the demand of refrigeration $\left(\dot{Q}_{need}(t)\right)$, and the hybrid cycle's operation mode is decided according to this criterion.

For the absorption subcycle, two cases are considered when calculating the driving heat input to the generator, depending on whether or not the absorption part alone can satisfy the whole demand (14 or 15, respectively).

$$\dot{Q}_G(t) = \frac{\dot{Q}_{need}(t)}{COP^{ABS}} \qquad if \quad \dot{Q}_{E,\max}^{ABS}(t) \geq \dot{Q}_{need}(t) \quad (14)$$

$$\dot{Q}_G(t) = \dot{Q}_{in}(t) \qquad if \quad \dot{Q}_{E,\max}^{ABS}(t) < \dot{Q}_{need}(t) \quad (15)$$

Once the heat input to the generator is known, calculation of the useful cooling effect delivered at the evaporator by the absorption subcycle is straightforward (16).

$$\dot{Q}_E^{ABS}(t) = \dot{Q}_G(t) \cdot COP^{ABS} \quad (16)$$

Surplus heat produced by the solar system is derived to the thermochemical subcycle (17), causing some refrigerant to vaporize due to the reaction (18) and therefore storing some cooling capacity in

form of liquefied refrigerant (19), which can be later utilized. When calculating the amount of refrigerant being vaporized at the reactor, a value is needed for the enthalpy of reaction (Δh_R); for reactions involving ammonia, a standard value of 40 kJ/(mole of NH_3) can be assumed as an approximation. Since all the demand is being covered by the absorption subcycle in this period, no cooling effect needs to be provided by the thermochemical subcycle (20).

$$\dot{Q}_R(t) = \dot{Q}_{in}(t) - \dot{Q}_G(t) \qquad if \quad \dot{Q}_{E,\max}^{ABS}(t) > \dot{Q}_{need}(t) \tag{17}$$

$$\dot{m}_r^{TCH}(t) = \frac{\dot{Q}_R(t)}{\Delta h_R} \qquad if \quad \dot{Q}_{E,\max}^{ABS}(t) > \dot{Q}_{need}(t) \tag{18}$$

$$m_r^{TCH}(t) = m_r^{TCH}(t-1) + \dot{m}_r^{TCH}(t) \cdot \Delta t \qquad if \quad \dot{Q}_{E,\max}^{ABS}(t) > \dot{Q}_{need}(t) \tag{19}$$

$$\dot{Q}_E^{TCH}(t) = 0 \qquad if \quad \dot{Q}_{E,\max}^{ABS}(t) > \dot{Q}_{need}(t) \tag{20}$$

The other way around, when the absorption subcycle alone cannot satisfy the demand, some cooling effect has to be provided by the thermochemical part (21). Some of the stored refrigerant is vaporized (22), being therefore destored (23), and also rejecting heat at the reactor (24).

$$\dot{Q}_E^{TCH}(t) = \dot{Q}_{need}(t) - \dot{Q}_E^{ABS}(t) \qquad if \quad \dot{Q}_{E,\max}^{ABS}(t) < \dot{Q}_{need}(t) \tag{21}$$

$$\dot{m}_r^{TCH}(t) = \frac{\dot{Q}_E^{TCH}(t)}{\Delta h_V} \qquad if \quad \dot{Q}_{E,\max}^{ABS}(t) < \dot{Q}_{need}(t) \tag{22}$$

$$m_r^{TCH}(t) = m_r^{TCH}(t-1) - \dot{m}_r^{TCH}(t) \cdot \Delta t \qquad if \quad \dot{Q}_{E,\max}^{ABS}(t) < \dot{Q}_{need}(t) \tag{23}$$

$$\dot{Q}_R(t) = \frac{\dot{Q}_E^{TCH}(t)}{COP^{TCH}} \qquad if \quad \dot{Q}_{E,\max}^{ABS}(t) < \dot{Q}_{need}(t) \tag{24}$$

For periods where the absorption subcycle can provide exactly the amount of cold demanded, $\dot{Q}_R(t)$, $\dot{Q}_E^{TCH}(t)$ and $\dot{m}_r^{TCH}(t)$ become zero.

In any case it must be always verified that the total useful cooling effect delivered at the evaporator is the sum of that of the absorption part and that of the thermochemical part (25). In case the system is not designed to cover 100% of the demand, an auxiliary heat source is needed (26).

$$\dot{Q}_E^{HYB}(t) = \dot{Q}_E^{ABS}(t) + \dot{Q}_E^{TCH}(t) \tag{25}$$

$$\dot{Q}_E^{TOT}(t) = \dot{Q}_E^{HYB}(t) + \dot{Q}_E^{AUX}(t) \tag{26}$$

5. Results and discussion

In this section, the main results of the cycle preliminary simulation are shown.

In Fig.4 it can be seen that in those periods where surplus heat is provided by the solar system, the amount of cooling capacity associated to liquid refrigerant in the reservoir increases. The opposite situation happens when not enough solar radiation is available (for instance in day 3, which could represent a cloudy or rainy day). It can be noted that, while the absorption part of the cycle works when the solar system produces heat, the thermochemical process comes into scene as soon as the absorption refrigeration effect cannot handle the demand. Whether or not the hybrid cycle can fully satisfy the demand uninterruptedly, will mainly depend on design issues, being the amount of refrigerant in the thermochemical subcycle (which is the only one providing storage function) and collector field area the two most important ones. In this example case, the dimensioning of the system was done to obtain a solar fraction of 0.8 during one full month. It can be seen that the thermochemical subsystem has a maximum value of energy stored, which depends on the dimensioning of the system. To attain the abovementioned solar fraction in this case, a capacity of storage of 5 kWh of cooling effect would be needed, with 9 solar thermal collectors. Since solar coverage is < 1, an auxiliary heat source would be needed for the system in this example.

Fig. 5 shows the improvement in the system's performance which can be obtained by coupling the thermochemical subsystem to the absorption subsystem in the example shown above. As it can be seen, for a low number of solar collectors there is no big difference between running the hybrid system or just an absorption system alone. As the number of collector increases, more surplus heat is available for storage, and therefore the use of the thermochemical subsystem has more impact. However, the COP of the hybrid system becomes lower, because the thermochemical part gets more presence in the operation and its COP is lower than that of the absorption subsystem. The maximum CSD of the ABS subsystem is limited at <1 because of the mismatch between availability and demand; the maximum CSD of the HYB system could be eventually 1, depending on the number of collectors, and on the mass of refrigerant at the thermochemical subsystem.

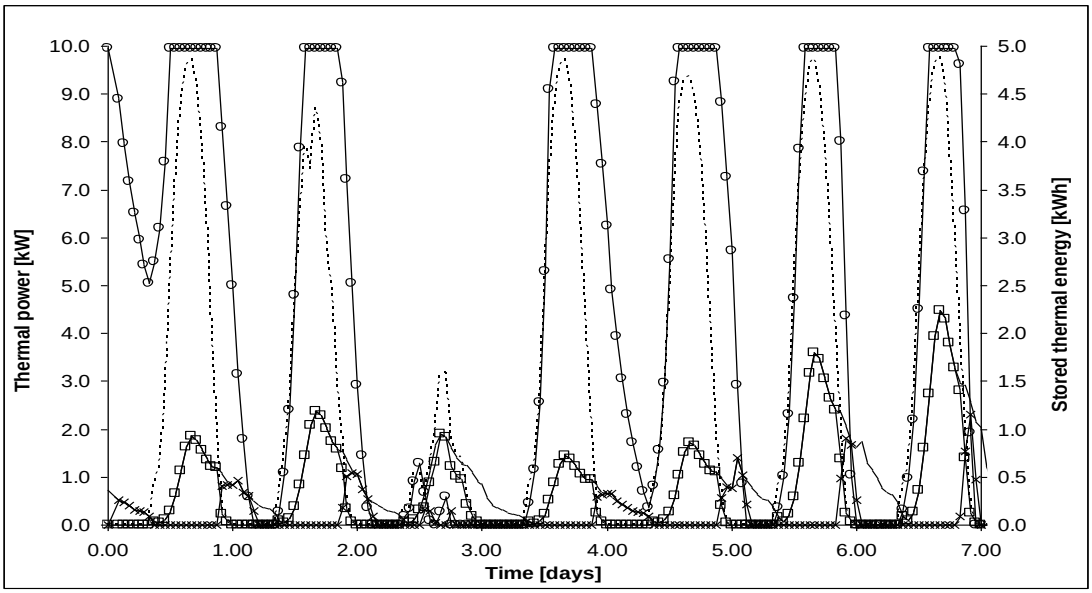

Fig. 4. Driving heat provided by solar system (dotted line, left axis), demand of cooling (straight line, left axis), cooling provided by the absorption subsystem (squared line, left axis) and by the thermochemical subsystem (crossed line, left axis) and stored cooling capacity associated to liquid refrigerant at the reservoir (circle line, right axis); profiles for one week in the example case.

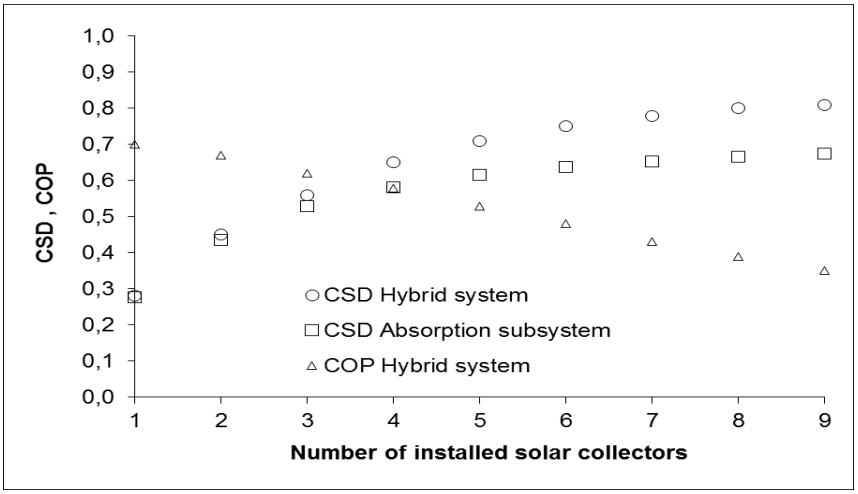

Fig. 5. Example scenario: performance indicators of the system for different number of installed solar thermal collectors, until reaching a desired coverage of 80% with 9 collectors.

6. Conclusions

A new solar cycle for refrigeration applications has been proposed and described. Its strengths and drawbacks, as well as suitable working pairs have been discussed, and a preliminary simulation for a residential cooling application has been carried out. The results show that the hybrid system offers

a potential improvement in mismatch compensation and demand coverage with respect to those of an absorption system alone.

Nomenclature

A useful area, m^2

CDD Cooling Degree Days, $^0C \cdot day$

COP Coefficient Of Performance

CSD Coefficient of Satisfaction of the Demand

h Enthalpy, kJ/mole of gas

k redistribution factor

m mass, kg

q specific monthly residential cooling demand, $kWhc/m^2/month$

Q heat, kJ

$\dot{Q}$ thermal power, kW

t time, h

T temperature, ^0C

Greek symbols

α utilization factor

β weekend correction factor

Δ variation

η efficiency

Subscripts and superscripts

0 Initial state

A Absorber

ABS Absorption subcycle

amb Ambient

b Base temperature

floor Residence floor

h Hourly

HYB Global hybrid cycle

in Input to the hybrid cycle

m Monthly

max Maximum

n Final state

need Demand of cooling

r Refrigerant

R Thermochemical reaction

rad Solar radiation

solar Solar system

TCH Thermochemical subcycle

wd Work day

we Weekend

References

[1] Pinel P., Cruickshank C. A., Beausoleil-Morrison I., Wills A. (2011). A review of available methods for seasonal storage of solar thermal energy in residential applications. *Renewable and Sustainable Energy Reviews 15*, 3341-3359.

[2] Mette B., Kerskes H., Drück H. (2012). Concepts of long-term thermochemical energy storage for solar thermal applications – Selected examples. *Energy Procedia 30*, 321-330.

[3] Cot-Gores, J., Castell, A., Cabeza, L. F. (2012). Thermochemical energy storage and conversion: A-state-of-the-art review of the experimental research under practical conditions. *Renewable and Sustainable Energy Reviews, 16*(7), 5207–5224.

[4] Mauran, S., Lahmidi, H., Goetz, V. (2008). Solar heating and cooling by a thermochemical process. First experiments of a prototype storing 60kWh by a solid/gas reaction. *Solar Energy, 82*(7), 623–636.

[5] Kerskes, H., Mette, B., Bertsch, F., Asenbeck, S., Drück, H. (2012). Chemical energy storage using reversible solid/gas-reactions (CWS) – results of the research project. *Energy Procedia 30*, 294-304.

[6] Kim, D. S., & Infante Ferreira, C. A. (2008). Solar refrigeration options - a state-of-the-art review. *International Journal of Refrigeration 31*(1), 3–15.

[7] Lahmidi H., Mauran S., Goetz V. (2006). Definition, test and simulation of a thermochemical storage process adapted to solar thermal systems. *Solar Energy 80,* 883-893.

[8] Li, T.X., Wang, R.Z., Li, H. (2014). Progress in the development of solid-gas sorption refrigeration thermodynamic cycle driven by low-grade thermal energy. *Progress in Energy and Combustion Science 40*, 1-58.

[9] Wang L.W., Wang R.Z., Oliveira R.G. (2009). A review on adsorption working pairs for refrigeration. *Renewable and Sustainable Energy Reviews 13*, 518-534.

[10] Wang, L.W., Wang, R.Z., Wu, J.Y., Wang, K. (2004). Compound adsorbent for adsorption ice maker on fishing boats. *International Journal of Refrigeration 27*, 401-408.

[11] Stitou D., Mazet N., Mauran S. (2012). Experimental investigation of a solid/gas thermochemical storage process for solar air-conditioning. *Energy 41*, 261-270.

[12] Pons M., Anies G., Boudehenn F., Bourdoukan P., Castaing-Lasvignottes J., Evola G., Le Denn A., Le Pierrès N., Marc O., Mazet N., Stitou D., Lucas F. (2012). Performance comparison of six solar-powered air-conditioners operated in five places. *Energy 46*, 471-483.

[13] Michel B., Mazet N., Neveu P. (2014). Experimental investigation of an innovative thermochemical process operating with a hydrate salt and moist air for thermal storage of solar energy: Global performance. *Applied Energy 129*, 177-186.

[14] Nowag J., Boudéhenn F., Le Denn A., Lucas F., Marc O., Raduslescu M., Papillon P. (2012). Calculation of performance indicators for solar cooling, heating and domestic hot water systems. *Energy Procedia 30*, 937-946.

[15] Dincer I., Rosen M. A., Exergy: Energy, Environment and Sustainable Development. New York: Elsevier; 2007.

[16] Lior N., Zhang N. (2007). Energy, exergy, and Second Law performance criteria. *Energy 32*, 281–296.

[17] Heller, A. (2000). Demand modelling for central heating systems. Report R-040, Department of Buildings and Energy. Technical University of Denmark (DTU). ISBN: 87-7877-042-4.

[18] Pedersen, L. (2007). Load modelling of buildings in mixed energy distribution systems [dissertation]. Trondheim, Norway: Norwegian University of Science and Technology NTNU; 2007.

[19] López Villada, J. Integración de sistemas de refrigeración solar en redes de distrito de frío y de calor [dissertation]. Tarragona, Spain: Universitat Rovira i Virgili, 2010.

[20] Garousi Farshi L., Infante Ferreira C.A., Mahmoudi S.M.S., Rosen M.A. (2014). First and second law analysis of ammonia/salt absorption refrigeration systems. *Int. J. Ref. 40*, 111-121.

[21] Le Pierrès N., Mazet N., Stitou D. (2007). Modelling and performances of a deep-freezing process using low-grade solar heat. *Energy 32*, 154-164.